The relationship between dynamics and structure in the far infrared absorption spectrum of liquid water

K.N. Woods, [1,*] & H. Wiedemann [2]

[1]*BioPhysics Program, Stanford University, Stanford, CA 94309*

[2]*Applied Physics Department and SSRL, Stanford University, Stanford, CA 94309*

Abstract

Using an intense source of far – infrared radiation, the absorption spectrum of liquid water is measured at a temperature ranging from 269 to 323 K. In the infrared spectrum we observe modes that are related to the local structure of liquid water. Here we present a FIR measured spectrum that is sensitive to the low frequency (< 100cm^{-1}) microscopic details that exist in liquid water.

Introduction

FIR spectroscopy is an experimental method that has been around for some time, but it is the recent existence of intense sources of far infrared radiation that has lead to its reemergence as an important tool for investigating the low frequency dynamics and local structure of complex liquids such as water. The SUNSHINE (Stanford University Short Intense Electron Source) facility at Stanford University is an example of a new generation source of FIR [1,2]. Producing coherent far infrared radiation with an energy of ~100 nJ per micro-pulse, the radiance greatly exceeds that of most blackbody or synchrotron radiation source and possibly offers information about low frequency intermolecular motions in liquids that has not been available from conventional sources.

[*] Corresponding author. Fax: 1-650-926-4100.
Email address: kwoods@stanford.edu

Work supported in part by the Department of Energy Contract DE-AC02-76SF00515
Stanford Linear Accelerator Center, Stanford University, Stanford, CA 94309

Therefore in this letter we will draw upon recent information gained from the results of other experimental techniques, with the aim of interpreting the absorption spectrum of water obtained from our own source of unique, very intense FIR.

In the last several years there has been a steady increase in the number of experimental methods that are capable of probing detailed characteristics related to the structural and dynamical properties of liquid water. These experiments are unique in the sense that they are just beginning to penetrate areas of investigation that have previously only been accessible through theoretical study and computer simulation. The information gained from these recent experiments has been indispensable in elucidating some of the complex interactions occurring in liquid water. In some cases, the results from these studies have been useful in confirming and even expanding on some of the ideas that had already been developed through more theoretical investigation. In other instances, they have lead to a constructive reconsideration about some of the more established ideas that have been associated with the properties of water.

Inelastic X-ray Scattering (IXS), Depolarized Raman, Mid Infrared, and THz spectroscopy are examples of experimental methods that are capable of probing the dynamics in liquid water. The dynamical properties of water are determined by both a fluctuating network of hydrogen bonds as well as by intermolecular interactions occurring between individual water molecules. Consequently, a precise interpretation of the underlying dynamics occurring in the liquid can be quite elusive regardless of the method used to study it. FIR spectroscopy does not differ in this respect. The low

frequency absorption spectrum consists of contributions from both permanent dipole moments in the system as well as from dipole induced dipole contributions that result from interactions between neighboring molecules. It is this aspect of FIR spectroscopy, the relationship between the dipole dynamics of the system to oscillations of stable structures within the same system that makes it a useful tool for monitoring motions and changes taking place about a reference molecule and its extended environment.

Experimental Methods

An electron beam pulse composed of a string of about 3000 equidistant 120 fs-rms bunches every 350 ps is produced at SUNSHINE. As the beam passes through a thin Al foil, far infrared Transition radiation is produced in the form of a Fourier transform limited radiation pulse of equal time structure. The spectral range is determined by the Fourier transform of the particle distribution and extends from $5cm^{-1}$ – $120cm^{-1}$. Each micropulse contains an energy of about 100 nJ.

The frequency dependent absorption coefficient of the double-distilled water samples is determined from a single, dispersive, interferometric measurement. The sample cell is composed of a polished silicon window that also serves as a reflector in one arm of the two-beam interferometer. In an experiment, the sample is placed on the backside of the cell window. When radiation enters into the interferometer, it is split into two parts by a 0.0254 mm thick Mylar beam splitter. One beam is reflected onto a moveable mirror and the other is transmitted through the beam splitter onto the sample cell. The portion of the beam that is transmitted onto the sample cell consists of a ray

reflected from the front surface of the silicon window and a delayed pulse reflected from the silicon-sample interface. At normal incidence, the Fourier-Transform of the ratio of these two signals can be related to complex Fresnel coefficients [3]. If the thickness and dielectric properties of the cell window are known, measurement of the frequency-dependent change in the amplitude and phase of the reflected signals allow the optical properties of the sample to be determined. For all of the measurements, a room temperature pyroelectric (Molectron $LiTaO_3$ P1-65 detector) is used to detect the coherent FIR signal. In each scan an average of 30 pulses is used for each individual data point in the interferogram and six independent scans are averaged together for each absorption measurement.

The *ab initio* molecular dynamic simulation is performed using the Car Parrinello method and the CPMD program [4]. Semi-local norm-conserving Martins-Troullier pseudopotentials are used for the core-valence interactions with a plane wave cut-off of 70 Ry and a gradient-corrected BLYP density functional [5,6]. The pseudopotential cut-off radii for O and H are 1.11 and 0.50 respectively. The fictitious mass associated with the plane wave coefficients is chosen to be 900 a.u., and the time step used to integrate the equations of motion is 0.120 fs. The system consists of a cubic box of 32 water molecules with periodic boundary conditions under ambient conditions and at experimental density. The infrared absorption coefficient is calculated using the dipole correlation function from the simulation and the following equation:

$$\alpha(\nu)\cdot n(\nu) = \frac{4\pi\nu\tanh(\beta\hbar\nu/2)}{3\hbar cV}\times\int_{-\infty}^{\infty} dt e^{-i\omega t}\langle \mathrm{M}(t)\cdot\mathrm{M}(0)\rangle, \qquad (1)$$

where $\alpha(\nu)$ is the frequency dependent absorption coefficient, $n(\nu)$ is the frequency dependent refractive index, $\beta=1/k_bT$ and k_b is Boltzmann's constant, V is the volume, T is the temperature, c is the speed of light in vacuum, and **M** is the total dipole moment obtained from the 6 ps simulation. Quantum corrections are taken into account only by the $\tanh(\beta\hbar\nu)/2$ factor in Equation (1) in the > 300 cm^{-1} spectral region. A more detailed treatment, as suggested by Guillot [7, 35], has been employed in the ≤ 300 cm^{-1} region.

Results and Discussion

An absorption mode around 45 - 50 cm^{-1} has been identified in Raman [8-10] and questionably in IR [3,11] spectroscopic experiments on water. Recent IXS experiments [12,13] have been extremely useful in confirming the importance of hydrogen bonding in determining the collective dynamics of liquid water and ice. A band close in frequency to the one found in IR and Raman experiments has also been observed in the Q > 1nm^{-1} region in IXS measurements of liquid water. This band has been interpreted as a restricted translational mode (O···O···O localized bending vibration) associated with a tetrahedral arrangement of water molecules about a central water molecule. In addition to the 50cm^{-1} mode, an additional temperature dependent band centered at about 70cm^{-1} has also been identified in low frequency Raman experiments [14]. The origin of this mode has been attributed to a secondary, weaker hydrogen- bonding environment that exists in liquid water that differs from the tetrahedral bonding arrangement that one would expect in hexagonal ice (I_h). With a noticeable increase in the strength of this band with increasing temperature, it has been suggested that this mode might be related to structural changes occurring within the hydrogen bond network in the liquid.

Experimental support for a heterogeneous mixture of hydrogen bonding types in liquid water has also been found using other experimental techniques. Femtosecond time resolved IR experiments [15], probing the orientational dynamics of the O-H stretching band in liquid water, have uncovered two distinct hydrogen bonding types in water: a weakly hydrogen bonded species associated with a fast relaxation time and a strongly bonded species with a much slower relaxation time. Subsequent THz dielectric response measurements [16] have also been consistent with a two-component structural model of water. In both of these studies, the underlying mechanism of the second relaxation process has been ascribed to a molecular relaxation associated with structural rearrangement within the weakly hydrogen bonded component.

In our temperature study of liquid water we find prominent absorption bands at 40, 55, 65, 80, and 90cm^{-1} at 269 K (Figure 1). As the temperature increases, the 40cm^{-1} band transforms into a barely discernable shoulder in the room temperature absorption spectrum. This mode disappears completely from the absorption spectrum above 298 K. Perhaps the most interesting trend in the temperature dependent absorption spectrum is the 55cm^{-1}mode found at 269 K. In the room temperature spectrum it is slightly red shifted in comparison to that of the supercooled liquid and appears at 49cm^{-1}. Above 298 K (Figure 2), this band remains at the same frequency but grows in intensity with an increase in temperature. The modes at 65, 80, and 90cm^{-1} at 269 K all move to lower frequency as the temperature is increased. In addition to the 49cm^{-1} mode, they are observed as a very broad peak centered about 70cm^{-1} in the 323 K spectrum.

In Figure 3 we find that our measured absorption spectrum of room temperature liquid water differs by as much as 40% when compared to the values reported in Reference 11 and in References 31 and 32. These differences are most apparent in the regions where we also find well resolved absorption bands in the water spectrum. Measurements have also been carried out on the absorption spectrum of the silicon window used in the experiments. We do not find significant absorption from the window in the region of the spectrum being investigated in this study; therefore, it seems unlikely that the absorption bands in our water spectra originate from the window.

Using a molecular dynamics simulation to study a model system of water, Errington and Debenedetti established a relationship between the translational order and orientational order in liquid water [17]. Their study revealed that these two properties are inherently coupled through H-bonding. The coupling was found to determine both the orientation of individual water molecules as well as their relative separation. In this same work, a plot of the distribution of hydrogen bonding environments revealed a structured and unstructured arrangement of water molecules that have a population distribution dependent on the temperature of the system. The results from this study would also seem to imply that the interaction potential between water molecules is also a variable function of temperature. In our experimental FIR absorption spectrum, we observe a red shift of mode frequencies with an increase in temperature. This trend is consistent with a lengthening or softening of hydrogen bonds in the system [18,19].

A more detailed view relating to the local geometric arrangement of water has been emerging from recent X-ray absorption spectroscopy (XAS) experiments [20,21]. With XAS it is possible to obtain direct information about the 3-D local coordination of water; such detailed information about the local configuration has not been available from radial distribution function data derived from neutron and X-ray diffraction studies. Results from these experiments indicate that room temperature water consists of a very unsaturated H-bonding environment. And a large percentage of water molecules in liquid water have free hydrogen bonds. This experimental work supports earlier theoretical studies that suggested that clusters and ring like structures are a dominant topology in room temperature water [22,23]. Fascinatingly, far infrared vibrational rotational tunneling (VRT) spectroscopy measurements have identified low frequency torsional motions involving the flipping of free hydrogen atoms in isolated water clusters [24,25]. These motions are observed in the $< 100 cm^{-1}$ region of the far infrared spectrum. It is interesting to speculate whether these types of intermolecular vibrations might also have a significant contribution in bulk water. Coincidently, we find some IR absorption modes in our experimental spectrum at frequencies similar to those reported in VRT spectroscopy studies. It is difficult to speculate about their origin, but these modes are seemingly not correlated with motions (torsions or bending) of molecules with the predicted symmetry of water in an "ice-like" or tetrahedral configuration [26,27].

To gain a deeper understanding about the microscopic dipole dynamics occurring in our experimental system, we have also used a density functional theory (DFT) based *ab initio* MD method to study room temperature liquid water. Previous DFT based studies have

successfully reproduced the IR absorption spectrum of water [28, 29]. We have implemented this method in an attempt to avoid some of the difficulties associated with approximations of the electronic part of the polarization that are commonly used in empirical models. Using the total dipole moment obtained from the *ab initio* MD trajectory, a plot of the calculated IR absorption spectrum of the water system is shown in Figure 4. The O-H intermolecular stretching mode, found at about 180cm^{-1} experimentally (at 298 K) [30, 3], is observed at about 200cm^{-1} in the calculated spectrum. The liquid water librational mode and the bending mode are also found in the first principles spectrum at about 630cm^{-1} and 1650cm^{-1} respectively.

Although there is less intensity in the < 100cm^{-1} region of the computed absorption spectrum, this region also provides information about intermolecular interactions occurring in the liquid water system. Furthermore, it coincides with the spectral region that we are able to access in our experimental FIR measurements; therefore, it will be considered in greater detail. In Figure 5b the total dipole spectrum from the simulation in the 10 – 100cm^{-1} region is shown. For this analysis, the spectrum has been separated into components relating to the water molecule principal axes to aid in the interpretation of the low frequency peaks found in the absorption spectrum. In the < 100 cm^{-1} region, there is a broad intermolecular peak centered at about 65cm^{-1}. Based on its correlation with motions involving both the x and z components of the molecular axis, it is probable that the 65 cm^{-1} peak is associated with a torsional motion occurring in the water network. In the direction representing motions in the molecular plane (y - axis) there is a prominent peak at approximately 85 cm^{-1} in the computed spectrum. Again

considering the molecular geometry of the molecules in the simulation system, this band is most likely related to dynamics taking place in the H –bonding network of the liquid water system. Although less prominent in the absorption spectrum, it is interesting to note that there is also a weak shoulder in the < 60cm^{-1} region of the CPMD spectrum that is attributed to motions normal to the molecular plane (x – axis). This band is very broad, but peaks at about 40cm^{-1} in the room temperature absorption spectrum. It is close in frequency to a peak that has been reported in experimental and theoretical studies on ice and supercooled liquid water [33,34]. And based on its directional contribution in the molecular reference frame, the 40 cm^{-1} absorption band in the computed spectrum is also consistent with the O···O···O bending assignment of the peak observed in those studies.

In summary, we have used an ultra-intense source of FIR to probe a region of the spectrum that is experimentally difficult to access. In our preliminary results we observe absorption modes that possibly offer new insight into the low frequency IR intermolecular dynamics and microstructure of liquid water. Future research will focus on isotope replacement studies that should be useful in confirming the origin of some of the absorption modes observed in this study.

Acknowledgements

This work was funded by the US Department of Energy, Basic Energy Science Contract No. DE-AC03-76SF00515. We thank the staff at SSRL and the Hansen Experimental Physics Laboratory for continued technical assistance while this experimental work was being carried out and the Center for Biomedical Computation at Stanford University for the allocation of computational time.

References

1. P. Kung, H. Lihn, & H. Wiedemann, Phys. Rev. Lett. 73 (1994) 967.
2. H. Lin, D. Bocek, C. Settakorn, & H. Wiedemann, Phys. Rev. E 53 (1996) 6413.
3. J.B. Hasted, S.K. Husain, F.A.M. Frescura, J.R. Birch, Chem. Phys. Lett. 118 (1985) 622.
4. R. Car & M. Parrinello, Phys. Rev. Lett. 55 (1985) 2471.
5. A.D. Becke, Phys. Rev. A 38 (1988) 3098.
6. C. Lee, W. Yang, R.C. Parr, Phys. Rev. B 37 (1988) 785.
7. Bertrand Guillot, J. Chem. Phys. 95(3) (1991) 1543.
8. K. Mizoguchi, Y. Hori, & Y. Tominga, J. Chem. Phys. 97 (1992) 1961.
9. J.L. Rousset, E. Duval, A. Boukenter, J. Chem. Phys. 92 (4) (1990) 2150.
10. G.E. Walfren, M.S. Hokmabadi, Y.C. Chu, B.J. Monosmith, J. Phys. Chem. 93 (1989) 2909.
11. Hans R. Zelsmann, Journal of Molecular Structure 350 (1995) 95.
12. M. Sampoli, G. Ruocco, F. Sette, Phys. Rev. Lett. 79 (1997) 1678.
13. G. Ruocco, F. Sette, J.Phys.: Condens. Matter 11 (1999) R259.
14. Y.C. Chu & G.E. Walrafen, in: M.-C. Bellissent-Funel, & J.C. Dore (Eds.), Hydrogen Bond Networks, Kluwer Academic Publishers, Netherlands, 1994, p. 169.
15. S. Woutersen & U. Emmerichs, Science 278 (1997) 658.
16. C. Rønne, P. Åstrand, S.R. Keiding, Phys. Rev. Lett. 82 (1999) 2888.
17. J. Errington & G. Debenedetti, Nature 409 (2001) 318.

18. A. Novak, Struct. Bonding 18 (1974) 177.

19. W. Mikenda, J. Mol. Struct. 147 (1986) 1.

20. U. Bergman, Ph. Wernet, P. Glatzel, M. Cavalleri, L. Petersson, A. Nilsson, S.P. Cramer, Phys. Rev. B 66 (2002) 092107-1.

21. S. Myeni, Y. Luo, L. Näslund, M. Cavalleri, L. Ojamäe, H. Ogasawara, A. Pelmenschikov, Ph. Wernet, P. Väterlein, C. Heske, Z. Hussain, L. Pettersson, A. Nilsson, J. Phys.: Condensed Matter 14 (2002) L213.

22. R. Ludwig & F. Weinhold, J. Chem. Phys. 110 (1999) 508.

23. Robin J. Speedy, J. Chem. Phys. 88 (1984) 3364.

24. K. Liu, M.G. Brown, J.D. Cruzan, R.J. Saykally, Science 271 (1996) 62.

25. Frank N. Keutsch & Richard J. Saykally, PNAS 98 (2001) 10533.

26. Noam Agmom, J. Phys. Chem. 100 (1996) 1072.

27. F.A. Cotton, Chemical Applications of Group Theory, Wiley and Sons, New York, 1990.

28. Pier Luigi Silvestrelli, M. Bernasconi, Michele Parrinello, Chem. Phys. Lett. 277 (1997) 478.

29. M. Sprik, J. Hutter, M. Parrinello, J. Chem. Phys. 105 (1996) 1142.

30. G.E. Walrafen & Y.C. Chu, J. Phys. Chem. 99 (1995) 11225.

31. George Hale & Marvin R. Querry, Applied Optics 12 (1973) 555.

32. M.N. Asar & J.B. Hasted, Infrared Physics 18 (1978) 835.

33. F. Sette, G. Ruocco, M. Krisch, C. Masciovecchio, R. Verbeni, U. Bergmann, Phys. Rev. Lett. 77 (1996) 83.

34. F. Sciortino, S. Sastry, J. Chem. Phys. 100 (5) (1993) 3881.

35. P.A. Egelstaff, Adv. Phys. 11, (1962) 203

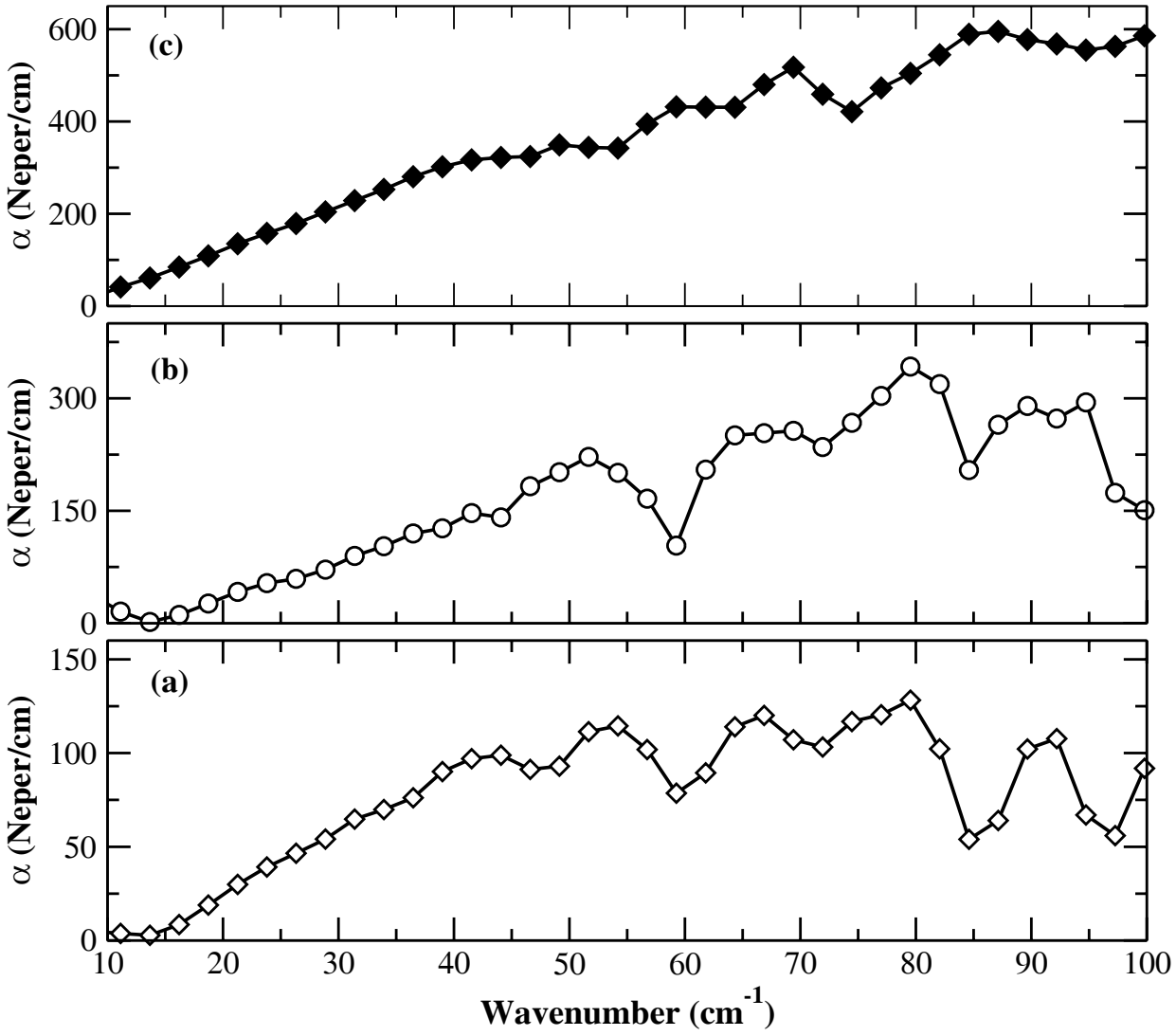
(c)
(b)
(a)
α (Neper/cm)
Wavenumber (cm-1)
0
200
400
600
150
300
50
100
10
20
30
40
50
60
70
80
90
100

Figure 1

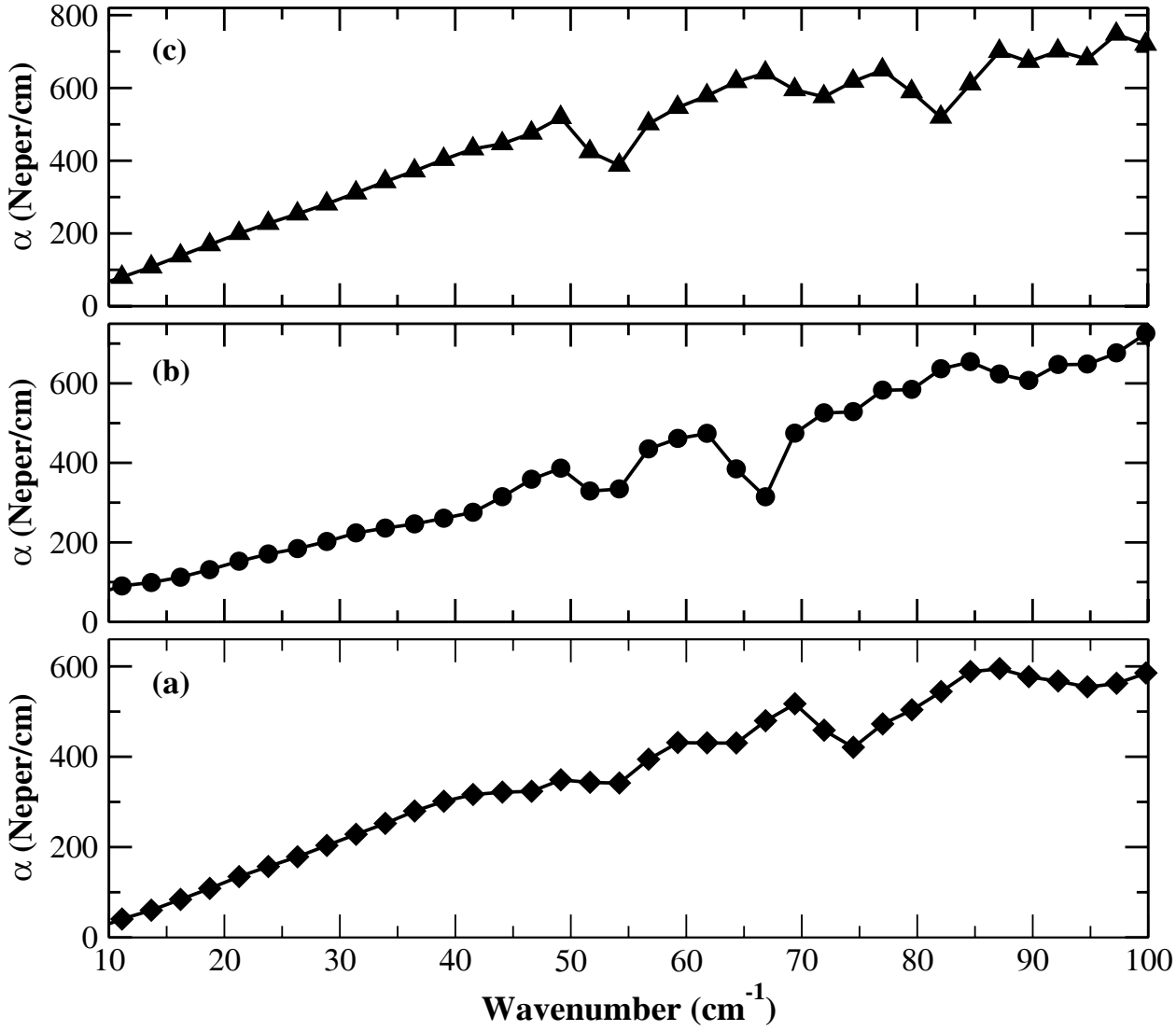
(c)
(b)
(a)
α (Neper/cm)
0
200
400
600
800
10
20
30
40
50
60
70
80
90
100
Wavenumber (cm-1)

Figure 2

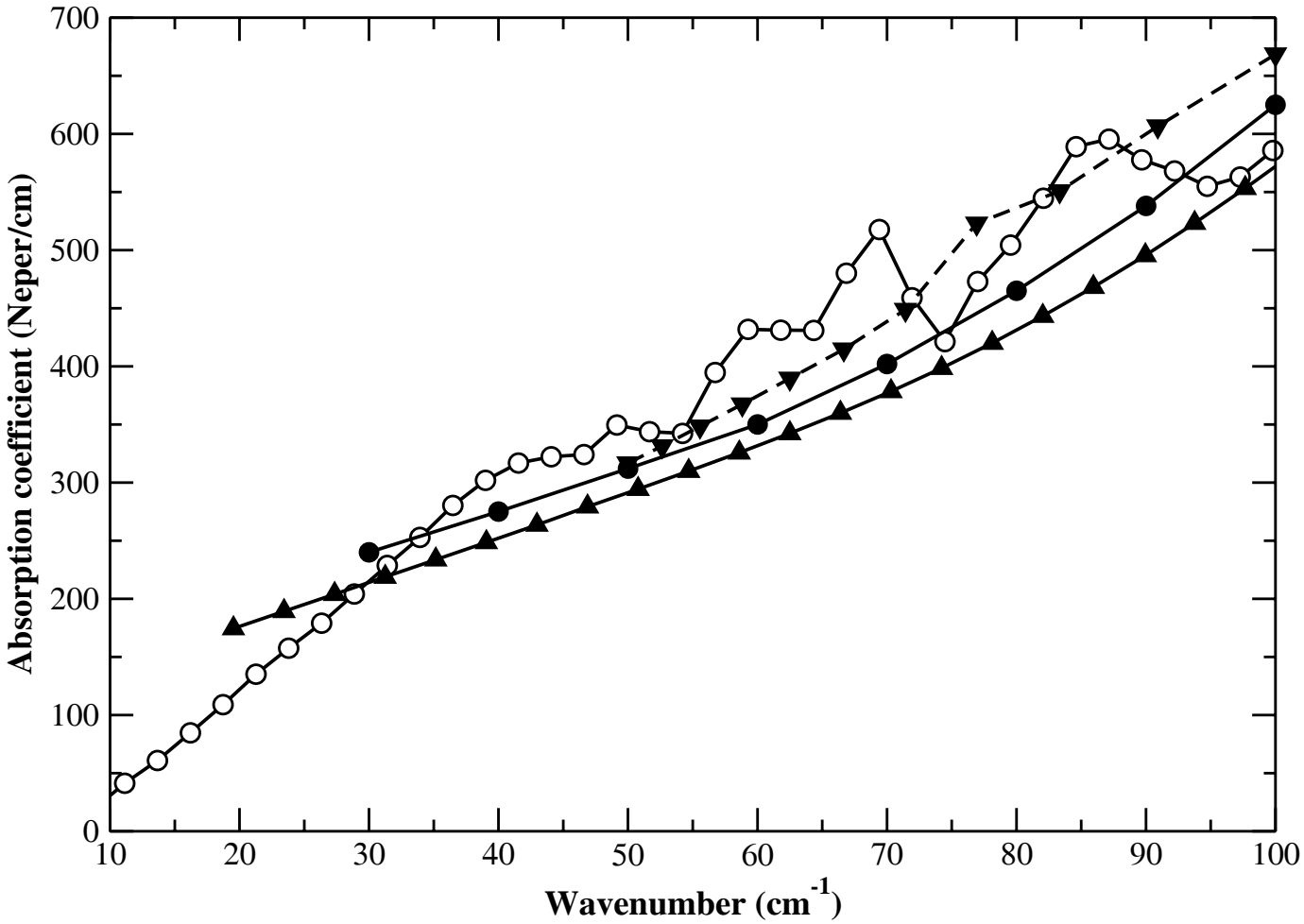
Absorption coefficient (Neper/cm)
Wavenumber (cm-1)
0
100
200
300
400
500
600
700
10
20
30
40
50
60
70
80
90
100

Figure 3

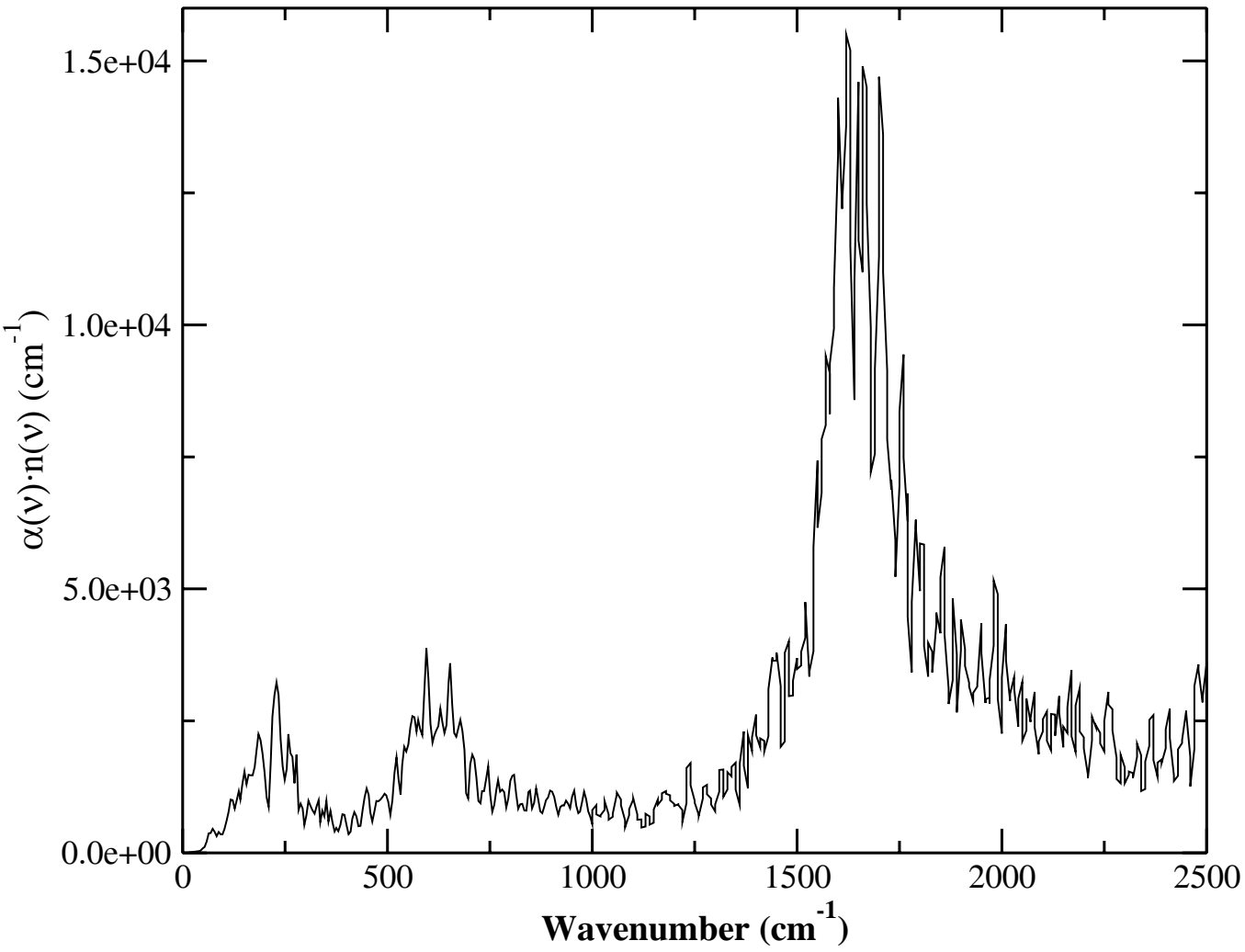
1.5e+04
1.0e+04
5.0e+03
0.0e+00
α(ν)·n(ν) (cm-1)
0
500
1000
1500
2000
2500
Wavenumber (cm-1)

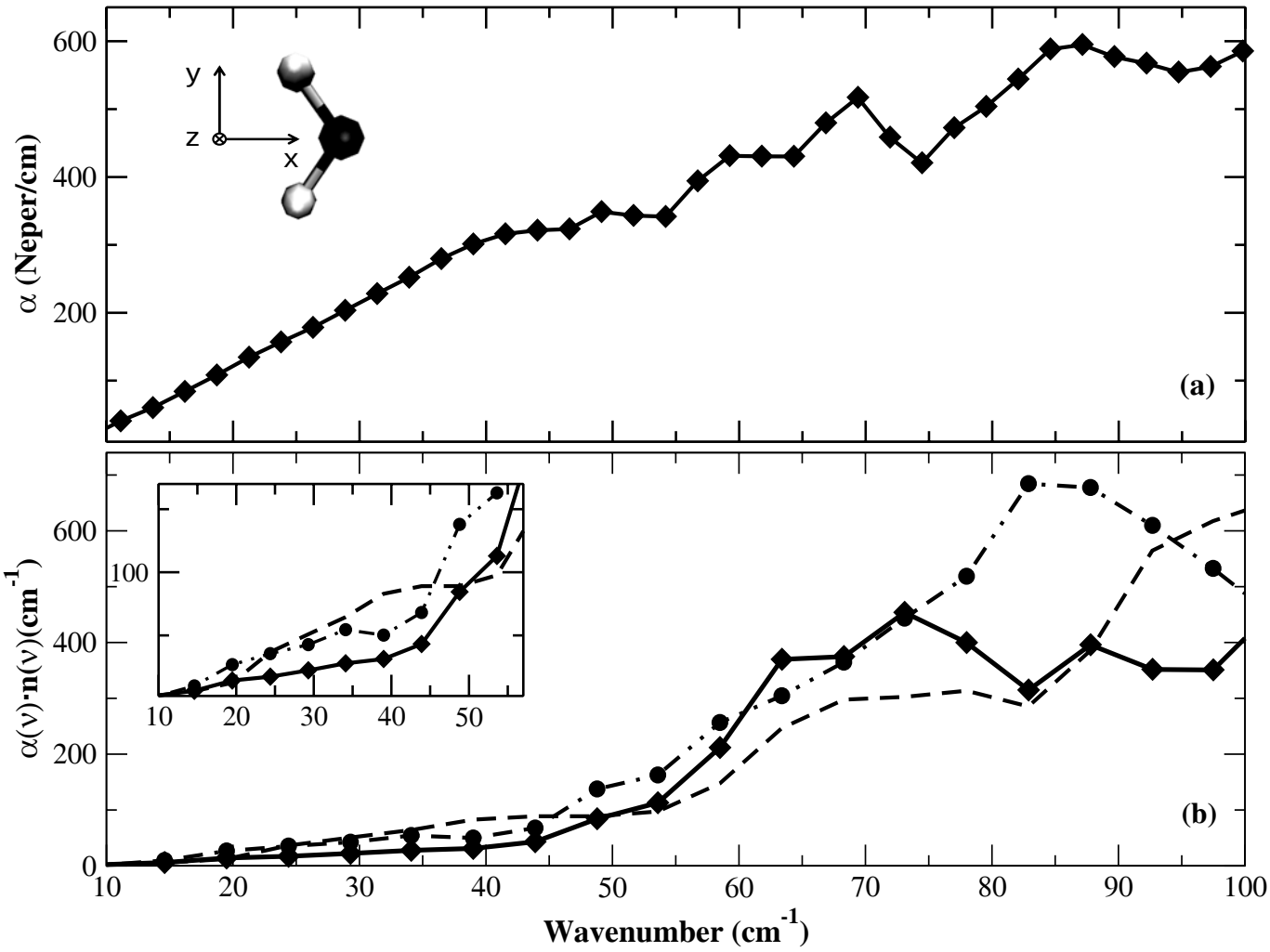
600
400
200
α (Neper/cm)
y
z
x
(a)
600
400
200
0
α(ν)·n(ν)(cm-1)
100
10
20
30
40
50
(b)
10
20
30
40
50
60
70
80
90
100
Wavenumber (cm-1)

Figure 5

Figure 1:

Experimental absorption spectrum of liquid water from 269 K – 298 K

(a) 269 K (open diamonds)

(b) 277 K (open triangles)

(c) 298 K (filled diamonds)

Figure 2:

Experimental absorption spectrum of liquid water from 298 K – 323 K

(a) 298 K (filled diamonds)

(b) 308 K (filled circles)

(c) 323 K (filled triangles)

Figure 3:

Experimental absorption spectrum of room temperature water from this study (solid line with open circles) and the experimental values taken from Ref. 31 (dashed line with filled right facing triangles); Ref. 32 (solid line with filled circles); and Ref. 11 (solid line with filled left facing triangles).

Figure 4: Computed IR absorption spectrum of room temperature H_20 using Eq. (1).

Figure 5:

(a) Experimental absorption spectrum of liquid water at 298 K. The principal axes reference frame of the water molecule is also shown in the upper left corner.

(b) The 10 – 100 cm^{-1} region of the computed IR absorption spectrum divided into components relating to the molecular principal axes. Dashed line: x – axis; dot – dot dashed line with filled circles: y – axis; and solid line with filled diamonds: z – axis. The inset shows the 10 – 55 cm^{-1} region of the computed spectrum.